Structure and Phase Composition of Deformed Heat-Affected Zone of the Weld Steel St3

Natalya Popova[1,2,a)], Aleksander Smirnov[3,4,b)], Elena Nikonenko[1,5,c)], Eugenii Ozhiganov[4,d)], Nina Koneva[1,e)], Eduard Kozlov[1]

[1]*Tomsk State University of Architecture and Building, 2 Solyanaya Square, Tomsk 634003 Russian Federation*
[2]*Institute of Strength Physics and Material Science SB RAS, 2/4 Akademichesky Avenue, Tomsk 634021 Russian Federation*
[3]*LLC "Kuzbass Center of Welding and Control", 33/2 Lenina Street, Kemerovo 650055 Russian Federation*
[4]*Kuzbass State Technical University, 28 Vesennyaya Street, Kemerovo 650000 Russian Federation*
[5]*National Research Tomsk Polytechnic University, 30 Lenina Avenue, Tomsk 634050 Russian Federation*

[a)]corresponding author: natalya-popova-44@mail.ru
[b)]galvas.kem@gmail.ru
[c)]vilatomsk@mail.ru
[d)]zhigan84@mail.ru
[e)]koneva@tsuab.ru

Abstract. The paper presents the transmission electron microscopy (TEM) investigations of the structural and phase conditions of the heat-affected zone of welded joint modified by plastic deformation. Tensile tests are carried out on INSTRON-1185 testing system at room temperature and 370 MPa loading. TEM investigations are carried out nearby the joint between the deposited and base metal, namely the type St3 steel. It is shown that the degree of plastic deformation has an effect on the material morphology, phase composition, defect structure and its parameters. It is shown that plastic deformation has no qualitative effect on the material structure, however it modifies its quantitative parameters. With the increase of the deformation degree, the perlite component becomes incomplete and transforms at first, to a fractured perlite and then to ferrite, thereby decreasing the volume ratio of perlite. The polarization of the dislocation structure is observed that, nevertheless, does not lead to the internal stresses that induce the specimen fracture.

INTRODUCTION

The technological development practically in all industries is currently impossible without welding, since the majority of structutes contains welded joints in their elements. The structural and phase condition of metal that is formed during welding, affects the mechanical-and-physical properties of products [1–4]. The modification of the structural and phase conditions in the course of operation and, especially, during deformation that often occurs in welded articles, can lead to adverse effects [2–4]. Therefore, the problems of the quality and reliability improvement of welded joints are still relevant nowadays. Thus, knowledge of the processes that define the formation and properties of welded joints underlies the solution of these problems. This knowledge relates to the joints between deposited and base metal, i.e. the heat-affected zones. Heat-affected zones is the most dangerous stress concentrator resulting in the formation of cracks and other defects [4], that considerably dcrease the strength and durability of welded articles [1–3]. Knowledge of the structural and phase conditions of the material and heat-affected zones in particular, provides not only the assesment of the strength properties of welded article but also the behavior of welded joint during the operation.

MATERIALS AND METHODS

Welded joint generated by the electrode welding was investigated in this experiment. The test machine INSTRON-1185 was used in this experiment to measure tensile strength of the steel specimen subjected to a quasi-static tensile deformation ranging from 0 to $\varepsilon = 5$ % under 370 MPa loading. Tensile stress testing was

Prospects of Fundamental Sciences Development (PFSD-2016)
AIP Conf. Proc. 1772, 030006-1–030006-7; doi: 10.1063/1.4964544
Published by AIP Publishing. 978-0-7354-1430-3/$30.00

accompanied by recording the acoustic emission and measuring the acoustic delay using the acoustic-surface-wave technique (Anstron) during the load achieving and removal [1, 2]. The investigations were carried out in the heat-affected zone (HAZ) in two points, namely: 1) base material at 1 mm distance from the joint between the deposited and base metals; 2) welded joint metal at 0.5 mm distance from the joint. The transmission electron microscopy (TEM) was used to investigate the structural and phase composition of the ultra thin specimens which were then studied on the electron microscope EM-125 operating at 125 kV accelerating voltage and having ×25000 magnification. The phase analysis was carried out using the TEM images supported by the micro-diffraction patterns and dark-field images obtained in the respective reflections [5, 6]. TEM images allowed obtaining such parameters as volume ratios P_V of the morphological components of the steel matrix; the size D of α-matrix fragments; scalar and excess dislocation densities ρ and $\rho_{\pm}$. All the parameters were measured by the standard techniques [7–9]. The experimental findings were statistically processed.

RESULTS AND DISCUSSION

The experiments show that in the original state (ε = 0), the matrices of the both base and welded joint metals are represented by α-phase, i.e. the solid solution of carbon and alloying elements in α-Fe phase having the bcc crystal lattice. Morphological components of α-phase are perlite and ferrite. TEM images of these components are presented in Fig. 1. Their volume ratios are different at ε = 0 in the base and welded joint metals (see Table 1). According to this Table, ferrite grains occupy the most of the volume ratio in heat-affected zones.

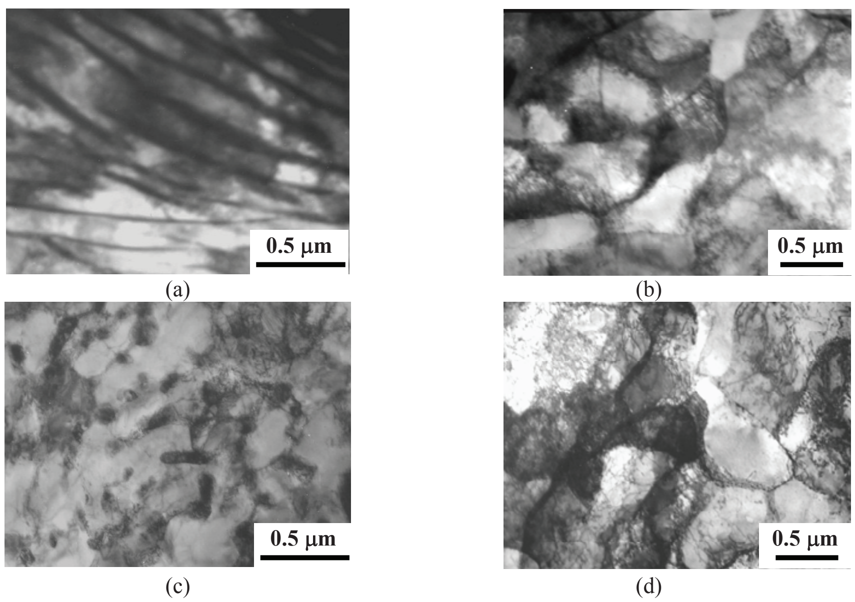

FIGURE 1. TEM images of heat-affected zones of welded joint. Original state: a,b) base metal; c,d) welded joint (a,c – perlite, b, d – ferrite).

TABLE 1. Quantitative variables of heat-affected zones of welded joint in the original state (ε = 0)

Quantitative variables	**Base metal**		**Welded joint metal**	
	Perlite	**Ferrite**	**Perlite**	**Ferrite**
Volume ratio	0.45	0.55	0.30	0.70
Fragment size in ferrite, μm		0.6 × 1.4		0.8 × 1.6
Scalar dislocation density ρ, cm^{-2}	$2.1\cdot10^{-10}$	$3.2\cdot10^{-10}$	$1.1\cdot10^{-10}$	$2.5\cdot10^{-10}$
Excess dislocation density $\rho_{\pm}$, cm^{-2}	$0.9\cdot10^{-10}$	$1.7\cdot10^{-10}$	$1.0\cdot10^{-10}$	$1.3\cdot10^{-10}$
Shear stress σ_s, MPa	330	360	210	320
Couple stress σ_c, MPa	230	265	200	225

The experiments show that perlite is lamellar. The dislocation structure of perlite is mostly represented by dense dislocation networks. The average scalar density ρ of dislocations is given in Table 1 for different portions of the material. The dislocation structure of perlite component is polarized that is indicated by the bend extinction contours in all ferrite layers in perlite. The values of the excess dislocation density $\rho_{\pm}$ measured by the width of the bend extinction contours are also given in Table 1.

According to Table 1, ferrite is fragmented as early as $\varepsilon = 0$. The size of fragments in the base metal is somewhat smaller than that in the welded joint. Inside these fragments, the network structure of dislocations is observed. The average scalar density of dislocations in ferrite grains is higher than in ferrite spaces. The dislocation structure is also polarized. According to the work of Utevsky [8], two types of stresses are detected, namely: 1) shear stress σ_s generated by the dislocation structure and 2) couple (local) stress σ_c generated by the excess dislocation density. The amplitudes of internal stresses are also given in Table 1. As it follows form this Table, the values of all parameters of the fine structure of the welded joint are less than in the base metal.

TEM images presented in Fig. 2 and Fig. 3 show that the deformation of the steel specimen does not lead to the qualitative changes in the structure, i.e. as before, it is represented by the ferrite and perlite mix component both in base metal and welded joint.

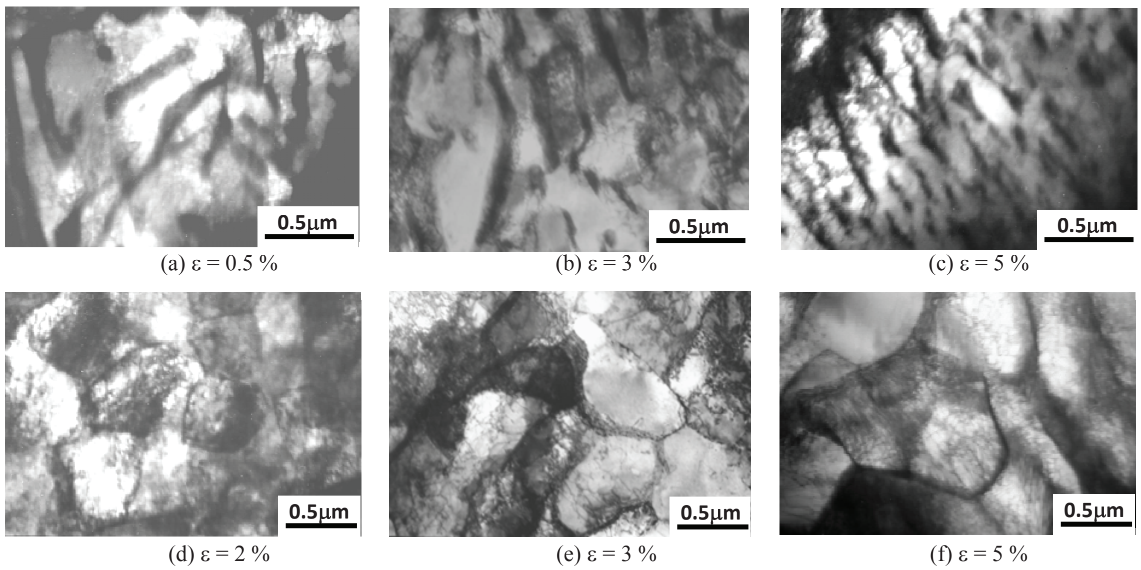

FIGURE 2. TEM images of heat-affected zones of modified welded joint.
Base metal: a, b, c – perlite, d, e, f – ferrite.

However, with the increase of the degree of plastic deformation ε, the volume ratio of the ferrite component matrix increases (Fig. 4a, 4b, curve 1), while that of perlite decreases (Fig. 4a, 4b, curve 2). According to this Figure, these modifications are greater in the metal of welded joint. Concurrently with the increase of the degree of plastic deformation ε, the lamellar perlite is gradually superseded by the fractured (Fig. 4c, 4d, curves 3-4). According to the curves 3-4 shown in Fig. 4c and Fig. 4d, the fragmentation of perlite in welded joint occurs more intensively.

With the increase of the degree of plastic deformation ε, the fragmentation of the ferrite grains is still observed, with more intensive one in the base metal. This results also in more intensive decrease of the average size of ferrite grains in the base metal with the increase of the degree of plastic deformation ε as compared to the welded joint metal (Fig. 5a, 5b). At the same time, in the base metal and welded joint alike the longitudinal size of fragments (curve 1) decreases more intensively than the crosswise size (curve 2).

Plastic deformation results in the decrease of scalar and excess dislocation densities ρ and $\rho_{\pm}$ in all areas of the specimen (Fig. 6). According to this Figure, with the increase of plastic deformation ε in the base metal, the average value of scalar dislocation density ρ increases insignificantly (Fig. 6a, curve 1). The increase of the excess dislocation density $\rho_{\pm}$ is more intensive, especially at the initial stage of deformation (Fig. 6a, curve 2). This is due to a significant increase of the volume ratio of ferrite grains as early as $\varepsilon = 0$ as compared to that of perlite grains. And it becomes larger with the increase of plastic deformation in ferrite (see Fig. 4a). Hence, the value and the behavior of ρ and $\rho_{\pm}$ in the material are defined by the ferrite component of the matrix, while their behavior in ferrite grains is similar to the behavior averagely in the whole material.

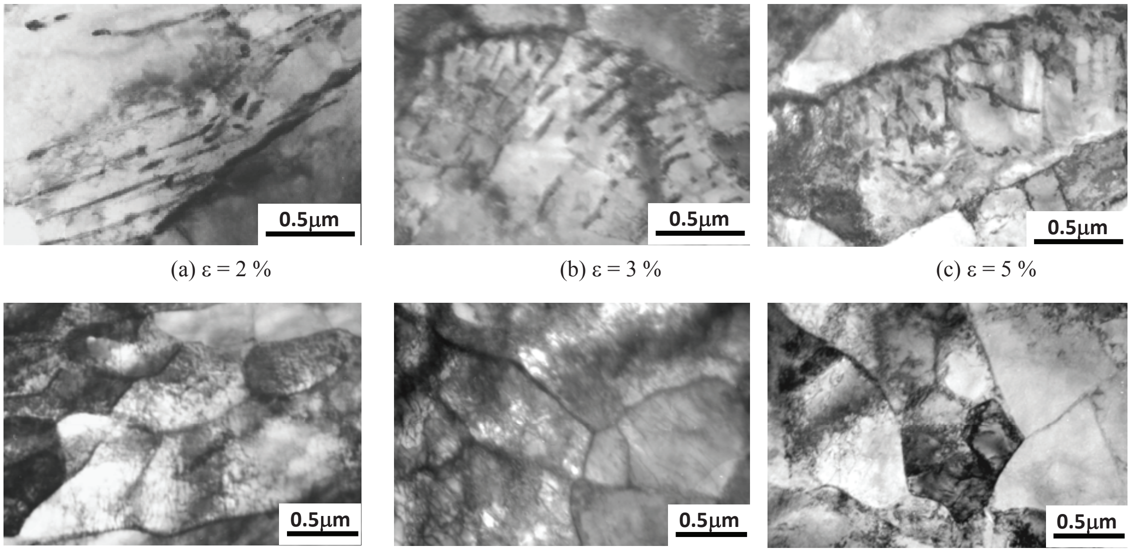

(a) ε = 2 % (b) ε = 3 % (c) ε = 5 %

(d) ε = 2 % (e) ε = 3 % (f) ε = 5 %

FIGURE 3. TEM images of heat-affected zones of modified welded joint.
Welded joint metal: a, b, c – perlite, d, e, f – ferrite.

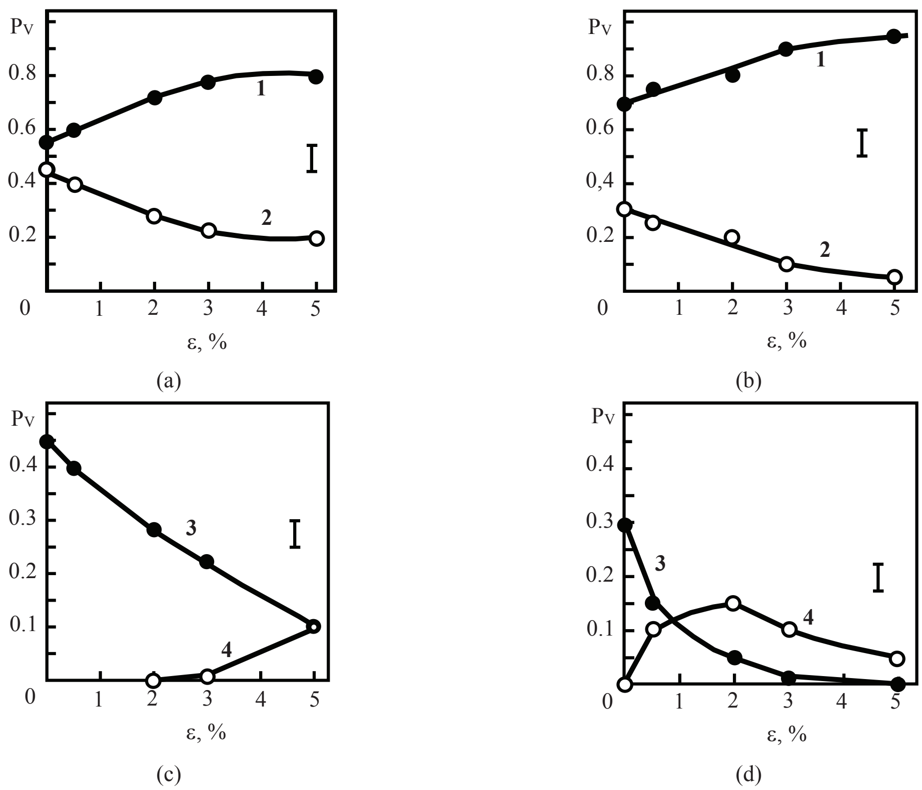

FIGURE 4. Volume ratios P_V depending on the degree of plastic deformation ε in heat-affected zones of St3 steel welded joint: a, c – base metal; b, d – welded joint; a, b – ferrite (1) and perlite grains (2); c, d – lamellar non-fractured (3) and fractured (4) perlite.

In welded joint metal, the average value of scalar dislocation density ρ increases rather non-uniformly with the increase of plastic deformation ε (Fig. 6b, curve 1). Thus, the rate of its growth at the initial stage of deformation is high (ε = 0–0.5%). Later it decreases (ε = 0.5–3%) and then practically stays unchanged (ε = 3–5%). The excess dislocation density $\rho_{\pm}$ uniformly increases with the increase of plastic deformation ε (Fig. 6b, curve 2). At the same time, at ε = 0, it was two times lower than scalar dislocation density ρ, while at ε = 5%, $\rho_{\pm} \approx \rho$. Both in welded joint and the base metal, the volume ratio of ferrite grains considerably exceeds that of perlite grains as early as ε = 0, and it grows with the increase of plastic deformation ε (see Fig. 4b). As a result, the value and the behavior of ρ and $\rho_{\pm}$ in welded joint is generally defined by the ferrite component, while their behavior in ferrite grains is similar to the behavior averagely in the whole material.

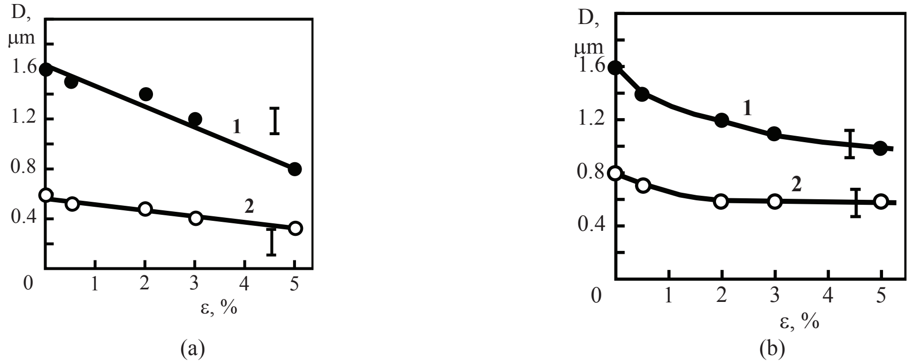

FIGURE 5. Average size D of ferrite fragments depending on degree of plastic deformation ε in heat-affected zones of St3 steel welded joint: a) base metal; b) welded joint; 1 – longitudinal size; 2 – crosswise size.

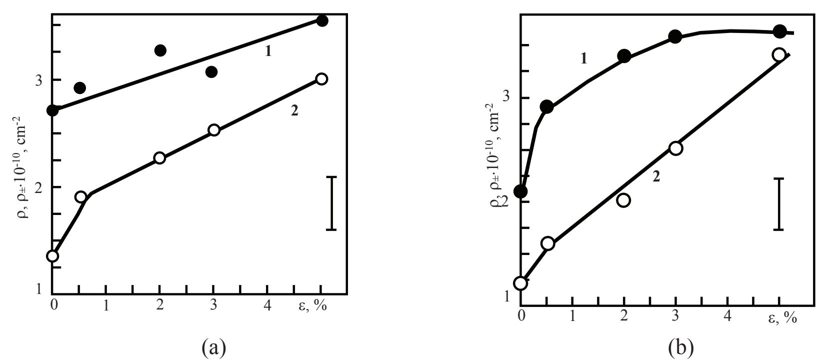

FIGURE 6. Dependencies between plastic deformation ε and dislocation structure: 1 – scalar density ρ; 2 – excess density $\rho_{\pm}$; a) base metal; b) welded joint.

Using the obtained ρ and $\rho_{\pm}$ values, the amplitudes of internal stresses σ_s and σ_c can be ascertained both averagely in the whole material and each morphological component of heat-affected zones matrix depending on the degree of plastic deformation. The obtained data are presented in the Fig. 7 and Fig. 8.

According to Fig. 7a and Fig. 8a, the average amplitude of shear stress σ_s modifies insignificantly with the increase of plastic deformation ε both in base metal and welded joint. Nevertheless, a tendency to its increase is observed.

The behavior of couple (local) stresses σ_c is different. From the very beginning of plastic deformation, its amplitude increases and stays lower than σ_s. During the formation of fractured perlite at ε = 3%, the value of σ_c increases and $\sigma_c > \sigma_s$. The behavior of σ_s and σ_c is different in different morphological matrix components, i.e. in ferrite and perlite grains. Thus, in ferrite grains (Fig. 7b, Fig. 8b), their average values well depend on the degree of plastic deformation, however, $\sigma_s > \sigma_c$ at $\rho > \rho_{\pm}$. It means that polarization of the dislocation structure does not lead to the internal stresses capable to destroy the specimen.

As shown in Fig. 7 c, 8 c, the behavior of σ_s and σ_c is changed. At plastic deformation of ε = 0–3 %, when lamellar perlite is not still fractured, the internal stresses increase at a similar rate, however, σ_s is higher than σ_c all the time. Within the deformation range of ε = 3–5 %, when the cementite lamels are fractured in perlite, σ_s/σ_c ratio is changed, i.e. σ_s is practically constant, while σ_c sharply increases and exceeds σ_s value ~1.5 times in base metal and more than twice in welded joint. It is the elastic component that contributes to σ_c value and its modification. With the increase of the degree of plastic deformation, this contribution grows, while the contribution from the plastic component is practically constant. And in the welded joint metal these changes are more notable. Such stresses must lead to cracking that is observed on TEM images of the microstructure. However, the volume ratio of perlite in the material (especially in welded joint) is rather insignificant. Hence, the formation of the main crack is not observed at ε = 5 %.

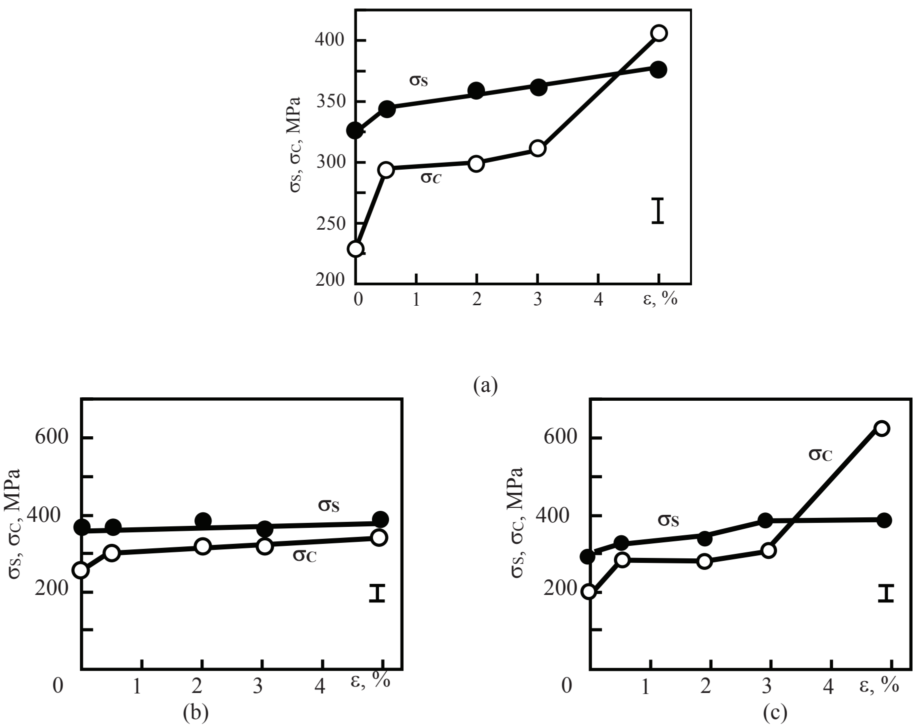

FIGURE 7. Dependences between plastic deformation ε and internal stresses σ_s and σ_c in heat-affected zones of St3 steel welded joint. Base metal: a) average values; b) ferrite; c) perlite.

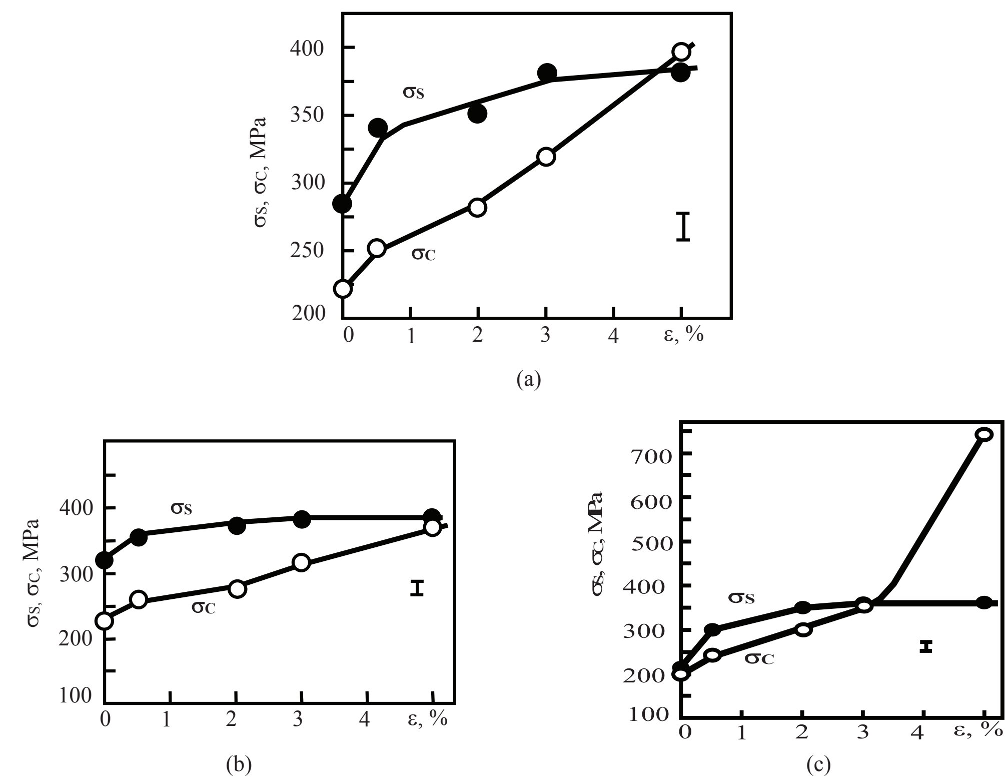

FIGURE 8. Dependences between plastic deformation ε and internal stresses σ_s and σ_c in heat-affected zones of St3 steel welded joint. Welded joint: a) average values; b) ferrite; c) perlite.

CONCLUSION

TEM investigations of the fine structure in heat-affected zones of welded joint in the type St3 steel produced by the electrode welding, showed that the morphological components of the steel matrix were partially represented by fractured lamellar perlite and fragmented ferrite both in the base metal and welded joint. The dislocation structure was partially polarized. The internal stress fields were not strong, i.e. the shear stress did not exceed 360 MPa in base metal and 320 MPa in welded joint; the couple stresses did not exceed 265 and 225 MPa, respectively. Tensile tests showed that the deformation range of $\varepsilon = 0–5\%$ resulted in perlite fracture and a further polarization of the dislocation structure. The amplitude of internal stress fields increased and $\sigma_c > \sigma_s$ at $\varepsilon = 5\%$. The elastic component provided the main contribution to σ_c value and its modification at $\varepsilon = 5$ %, thereby resulting in the formation of microcracks.

ACKNOWLEDGEMENT

This work was financially supported by Grant N 14-19-00724 from the Russian Science Foundation.

REFERENCES

1. L. P. Vishnyakov, V. P. Moroz, V. A. Pisarenko and A. V. Samelyuk, Powder Metall. Met. Ceram. **46**, 1–2, 38–42 (2007).
2. M. M. Rajath Hegde and A. O. Surendranathan, Powder Metall. Met. Ceram. **48**, 11–12, 641–651 (2009).
3. Ju. Hu, S. Wang, X. Zhao, S. Zhu and B. Yu, Front. Mech. Eng. China **5 (2)**, 189–193 (2010).
4. R. Ohashi, Weld. World **55**, 9–10, 2–11 (2011).
5. N. V. Boiko, I. A. Khazov, L. V. Selezneva, B. V. Bushmin, A. N. Semenov, G. V. Dubinin, S. N. Novozhilov and M. I. Plyshevskii, Met. Sci. Heat Treat. **54**, 9–10 (2013).
6. F. Foadian, M. Soltanieh and M. Adeli, Metal. Mater. Trans. A, **45A**, 4, 1823–1832 (2014).
7. M. Yu. Kollerov, S. D. Shlyapin, D. E. Gusev, K. S. Senkevich and Yu. E. Runova, Russ. Metall. **11**, 886–890 (2015).
8. V. P. Gagauz, E. V. Kozlov, V. I. Danilov, Yu. F. Ivanov and V. E. Gromov, *Structurally-phase state and mechanical properties of thick welded seams* (SSIU Publishing, Novokuznetsk, 2008) (in Russian) 150 p.
9. A. N. Smirnov, N. A. Koneva, S. V. Vollmer, N. A. Popova and E. V. Kozlov, *Defectiveness of welded joints. Spectral-acoustic method of control* (Mechanical Engineering, Moscow, 2009) (in Russian) 240 p.
10. A. N. Smirnov and E. V. Kozlov, *The substructure, internal stress field and the problem of the destruction of pipelines from steel 12Cr-1Mo-1V-Fe* (Kuzbassvuzizdat, Kemerovo, 2004) (in Russian) 163 p.
11. A. N. Smirnov, A. V. Ababkov, N. A. Koneva, E. V. Kozlov and N. A. Popova, Met. Sci. Heat Treat. **57**, 11–12, 752–758 (2016).
12. K. W. Andrews, D. J. Dyson and S. R. Keown, *Interpretation of Electron Diffraction Patterns* (Mir, Moscow, 1971) (in Russian) 256 p.
13. P. B. Hirsch, A. Howie, R. B. Nicholson, D. W. Pashley and M. J. Whelan, *Electron microscopy of thin crystals* (Mir, Moscow, 1968) (in Russian) 574 p.
14. V. S. Chernyavskii, *Stereology in metals* (Metallurgy, Moscow, 1977) (in Russian) 280 p.
15. L. M. Utevsky, *The diffraction electron microscopy in metal* (Metallurgy, Moscow, 1973) (in Russian) 583 p.
16. N. A. Koneva and E. V. Kozlov, “The physical nature of the plastic deformation staging” in *Structural levels of plastic deformation and fracture* (Nauka SB RAS, Novosibirsk, 1990) (in Russian) pp. 123–186.